Bioactive Non-Native Peptides

DOI: 10.1002/anie.201107011

Structurally Diverse μ-Conotoxin PIIIA Isomers Block Sodium Channel $Na_V1.4$**

*Alesia A. Tietze, Daniel Tietze, Oliver Ohlenschläger, Enrico Leipold, Florian Ullrich, Toni Kühl, André Mischo, Gerd Buntkowsky, Matthias Görlach, Stefan H. Heinemann, and Diana Imhof**

Voltage-gated sodium channels (VGSCs) play a key role in the electrical activity of neurons and of other excitable cells.[1] Certain VGSC subtypes ($Na_V1.3$, 1.7, 1.8, and 1.9) are expressed in the peripheral nervous system and mediate the transmission of signals leading to the sensation of different kinds of pain, such as nociception ($Na_V1.8$), acute inflammatory ($Na_V1.7$), and neuropathic ($Na_V1.3$) pain.[2] Therefore, VGSCs are potential targets for novel analgesics, ideally those with strong channel specificity. Among sodium channel antagonists, μ- and μO-conotoxins from the venoms of marine cone snails have attracted considerable attention because of their analgesic potency.[2a,3] μ-Conotoxins are 14- to 26-mer peptides with six cysteine residues (Supporting Information, Table S1).[4] They inhibit muscle and/or neuronal VGSCs by occluding the ion channel pore.[5] A specific cysteine framework, that is, $CCX_nCX_nCX_nCC$, confers conformational restriction to their three-dimensional structure upon formation of three disulfide bonds. It is generally accepted that the native fold of the toxins carries the disulfide connectivities Cys1–Cys4, Cys2–Cys5, and Cys3–Cys6 (numbered in the order of occurrence in the amino acid sequence).[3,5b] However, three-dimensional structures are available only for a limited subset of μ-conotoxins, that is, PIIIA,[6] GIIIA,[7] GIIIB,[8] TIIIA,[2c] SmIIIA,[9] SIIIA,[10] and KIIIA[11] (see also Table S1).

Concerning synthetic preparation of disulfide-bridged conopeptides, the most critical step certainly remains the oxidation to the correctly folded isomer, a process that usually becomes even more difficult with an increasing number of cysteine residues. For μ-conotoxins, which contain six cysteine residues, fifteen different disulfide-bridged isomers may be formed upon oxidation, even though certain conformations are suggested to be energetically favored.[12] Biological activity and structure of non-natively folded μ-conotoxin isomers has not been described to date, and the role of the disulfide connectivity pattern for activity is not yet clear. In contrast, the non-natively folded isomer of 15-mer α-conotoxin AuIB (two disulfide bonds) has been reported to have a nearly 10-fold greater potency than the native peptide.[13] This finding together with the greater complexity of conotoxins with three disulfide-bridges focused our attention on the representative μ-PIIIA from the cone snail *Conus purpurascens* (Figure 1).[5d,6,14]

We have elucidated the NMR solution structure of μ-PIIIA isomers obtained from synthetic material by oxidative folding in aqueous solution.[15] The reproducible formation of several disulfide-bridged peptide isomers was observed (Figure 1 a–c, Supporting Information, Figure S1). The three major components of the crude product, termed μ-PIIIA-1, -2, and -3 (**1**–**3**), were purified and subjected to further analysis (Supporting Information, Figure S2 and Tables S2–S5). The occurrence of different μ-PIIIA isomers in a mixture obtained from oxidative folding has been reported elsewhere, but structural analysis was not performed for these peptides.[14a,c]

Also, the solution structure of a synthetically produced μ-PIIIA has already been determined,[6] and the presence of a major and a minor conformation was discussed based on the occurrence of a *cis*/*trans* isomerization at the Phe7–Hyp8 and/or Lys17–Hyp18 peptide bond. However, the three-dimensional structure was only determined for the major isomer (protein data bank (PDB) code: 1R9I), while it was modeled for the minor isomer.[6]

The solution structure of μ-PIIIA isomers **1** and **2** (Figure 1 c) was determined by standard ^{1}H-based NMR spectroscopy. The good chemical shift dispersion of the backbone ^{1}H resonances for μ-PIIIA-1 and μ-PIIIA-2 allowed the unambiguous resonance assignment and provided a first indication of the well-defined structure of these peptides. Three of the four X-Hyp-peptide bonds in μ-PIIIA-1 and -2

[*] A. A. Tietze, T. Kühl, Prof. Dr. D. Imhof
Pharmaceutical Chemistry I, Institute of Pharmacy, University of Bonn, Brühler Strasse 7, 53119 Bonn (Germany)
E-mail: dimhof@uni-bonn.de
Dr. D. Tietze, Prof. Dr. G. Buntkowsky
Eduard Zintl Institute of Inorganic and Physical Chemistry
Technical University of Darmstadt
Petersenstrasse 20, 64287 Darmstadt (Germany)
Dr. O. Ohlenschläger, A. Mischo, Dr. M. Görlach
Biomolecular NMR Spectroscopy, Leibniz Institute for Age Research, Fritz Lipmann Institute, Beutenbergstrasse 11, 07745 Jena (Germany)
Dr. E. Leipold, F. Ullrich, T. Kühl, Prof. Dr. S. H. Heinemann
Department of Biophysics, Center for Molecular Biomedicine, Friedrich Schiller University of Jena and University Hospital Jena, Hans-Knöll-Strasse 2, 07745 Jena (Germany)

[**] We thank Prof. C. Hertweck (HKI Jena) for providing access to the MALDI TOF MS/MS instrument. This work was financially supported by the Friedrich Schiller University of Jena, by the State of Thuringia and the Federal Government of Germany. We thank Dr. U. Neugebauer (IPHT Jena) for Raman spectra.

Supporting information for this article is available on the WWW under http://dx.doi.org/10.1002/anie.201107011.

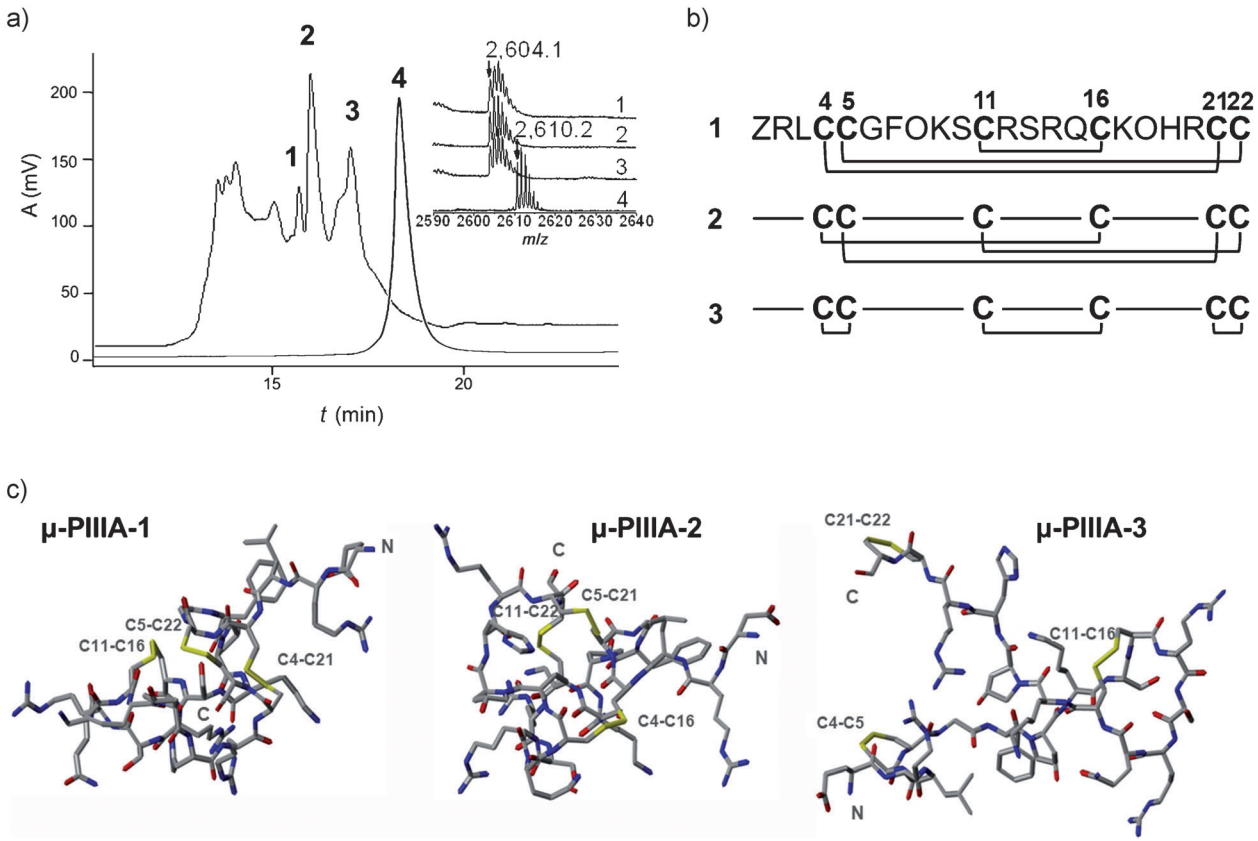

Figure 1. Studies of μ-PIIIA oxidation products. a) RP-HPLC chromatogram of μ-PIIIA obtained by oxidative folding in buffer with addition of GSH/GSSG at 4°C under argon atmosphere.[14c,15a,b] Elution carried out on a C18 Vydac column (250×4.6 mm) using solvents A (water/0.1% TFA) and B (acetonitrile/0.1% TFA), and the linear gradient: 10–40% of eluent B for elution. MALDI-TOF mass spectra of peptides **1** (μ-PIIIA-1), **2** (μ-PIIIA-2), and **3** (μ-PIIIA-3) and the linear precursor peptide **4**. The protonated $[M+H]^+$ peaks are marked at *m/z* 2610.20 Da for the reduced precursor and 2604.10 Da for the oxidized products. b) Three (1–3) out of 15 possible disulfide-bond connectivities representing the sequence of μ-PIIIA and numbering of cysteine residues within the sequence. Amino acid spacing between cysteine residues are assigned as loop regions. c) NMR solution structures of μ-PIIIA-1 (left) and μ-PIIIA-2 (center), and structural model for the extended μ-PIIIA-3 (right).

were assigned as *trans* based on a strong nuclear Overhauser effect (NOE) observed between the H^{α}_{i}–H^{δ}_{i+1} and absence of H^{α}_{i}–H^{α}_{i+1} cross peaks for both Phe7–Hyp8 and Lys17–Hyp18 peptide bonds, respectively. For μ-PIIIA-2, this assignment is consistent with the report of Nielsen and co-workers.[6] The solution structure of μ-PIIIA isomers **1** and **2** was calculated based on NOE data (Supporting Information, Table S5). The structure of either μ-PIIIA isomer is characterized by a rather compact global fold (Supporting Information, Figure S3 a,b) and their amino acids carrying long side chains (Leu, Arg) are pointing 'outwards' into the solvent (Figure 1 c). The overall structure is dissimilar (overall root mean squared deviation (r.m.s.d) 5.68 Å), however both share a α-helical element between Phe7 and Arg12, which superimpose with a backbone r.m.s.d. of 0.46 Å.

There are, however, significant differences between isoforms μ-PIIIA-1 and -2. The disulfide bond connectivities of the peptides were confirmed by examination of the NOEs between the cysteine residues. The disulfide bonds were between Cys4–Cys21, Cys5–Cys22, and Cys11–Cys16 for μ-PIIIA-1 as reflected by the intensity of the respective diagnostic NOE cross peaks Cys11H^{α}–Cys16H^{β} (medium), Cys11H^{α}–Cys16H^{N} (weak), and Cys5H^{α}–Cys22H^{β} (medium), whereas a rather different disulfide connectivity pattern (Cys4–Cys16, Cys5–Cys21, and Cys11–Cys22) was identified for μ-PIIIA-2 indicated by NOE cross peaks involving Cys4H^{β}–Cys16H^{β} (strong), Cys5H^{β}–Cys22H^{β} (weak), and Cys11H^{β}–Cys22H^{β} (strong). In contrast, the third isomer μ-PIIIA-3 appeared to be too flexible for structure determination as evident from the lower dispersion of proton resonances (Supporting Information, Figure S4). This greater flexibility is caused by a Cys4–Cys5, Cys11–Cys16, Cys21–Cys22 disulfide connectivity as determined by trypsin proteolysis and MALDI-TOF MS/MS (Supporting Information, Methods and Figure S5).

A closer look at the three isomer structures revealed that only μ-PIIIA-2 contains the cysteine framework described as typical for native μ-conotoxins. Thus, we assessed the biological activity of the μ-PIIIA isomers **1**–**3** (Figure 2, Supporting Information Figure S6) by measuring their potency of blocking skeletal muscle $Na_V1.4$ channels, expressed in HEK293 cells. Surprisingly, all three differently folded isomers blocked $Na_V1.4$-mediated ion currents measured electrophysiologically in the whole-cell patch-clamp

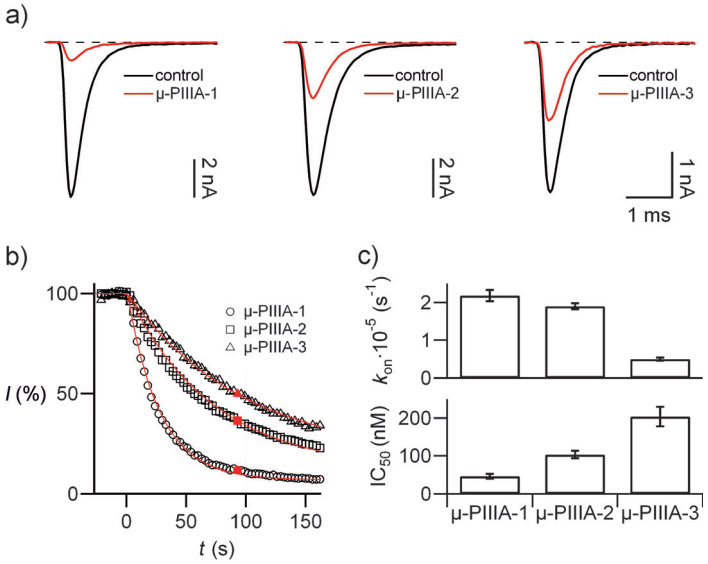

Figure 2. Blocking of sodium channels by μ-PIIIA isomers. $Na_V1.4$ sodium channels were transiently expressed in HEK293 cells and sodium currents were elicited with repetitive depolarizations to −10 mV. a) Representative current traces of before (control, black) and 90 s after application of 1 μM of the indicated μ-PIIIA isomers (red). b) Time course of normalized peak current reduction with toxin application at time zero. The continuous lines are single exponential data fits and the filled symbols indicate data points from the current traces shown in (a). c) Mean on-rate (k_{on}, top) and estimated IC_{50} values (bottom) for the indicated toxin isomers from experiments involving several different toxin concentrations (Supporting Information, Figure S6).

configuration. The inhibitory activity, determined from experiments involving various toxin concentrations (Supporting Information Figure S6), decreased in the following order: μ-PIIIA-1 > μ-PIIIA-2 > μ-PIIIA-3. The mean IC_{50} values were 46.7 ± 6.5 nM for μ-PIIIA-1, 103.2 ± 9.9 nM for μ-PIIIA-2, and 203.7 ± 25.7 nM for μ-PIIIA-3, while fully reduced μ-PIIIA was not active (not shown). This result also correlates with the circular dichroism (CD) data (Supporting Information, Figure S2) showing a decrease in folded conformation in the order μ-PIIIA-1 > μ-PIIIA-2 > μ-PIIIA-3 > reduced μ-PIIIA. These results clearly show that the unfolded μ-PIIIA precursor peptide cannot adopt an appropriate conformation to block the Na_V channel and that the fold of isomer **1** is preferred over the suggested native fold of isomer **2**. This situation indicates that μ-PIIIA-1 is more potent than the μ-PIIIA-2 isomer, which was proposed to represent the native fold.[6]

Members of the μ-family of conotoxins discriminate between Na_V channel subtypes, for example, μ-PIIIA is known to inhibit tetrodotoxin (TTX)-sensitive Na_V channels ($Na_V1.2$, $Na_V1.4$), displaying preference for skeletal muscle over nerve, moreover demonstrating a negligible effect on TTX-resistant Na_V channels ($Na_V1.5$).[2c,6,14b,c] Hence, understanding the molecular basis of μ-conotoxin channel selectivity is essential for the development of specific probes for VGSCs. In the context of recognition of ligand binding sites on the channel and in turn, elucidation of the mode of conotoxin action, investigations employing structures of voltage-gated potassium channels (VGPC) very recently attracted attention. For example, the complex of caribdotoxin (38-mer peptide with 6 cysteine residues) with the ion channel pore of KcsA (residues 1–132) investigated by NMR spectroscopy revealed a number of sites on the surface of the channel protein that were suggested to interact with the toxin in a lock-and-key fashion.[16] Another example is the kalitoxin (38-mer peptide with 6 cysteine residues)—KcsA channel $K_V1.3$ complex determined by solid-state NMR spectroscopy experiments.[17] Interestingly, these studies demonstrated that the rather long side chain of lysine-27 (K27) enters the channel pore, and that other amino acids (R24, N30) with long side chains additionally block the channel through interactions with specific residues on the extracellular side of the protein. This result led us to hypothesize about the activity of the different isomers of μ-PIIIA because μ-conotoxins all contain a conserved basic residue, lysine or arginine (R14 in μ-PIIIA), which is related to K27 in kalitoxin. A comparison of the structures of μ-PIIIA-1 and -2 indicated a higher similarity in the backbone region comprising amino acids 7–15, evident by an r.m.s.d. of 1.13 Å (Supporting Information, Figures S3, S7), where R14 (loop 2) is located. μ-PIIIA-2 shows high similarity to the NMR solution structure of μ-PIIIA[7b] (PDB ID: 1R9I, see Supporting Information, Figures S3, S7), in particular for the N-terminal residues 1–13. It exhibits an elongated and more regular α-helix when compared to $\mu\text{-PIIIA}_{1R9I}$ and superimposes with a backbone r.m.s.d. of 1.13 Å for residues 4–13. In contrast, for the same stretch, μ-PIIIA-1 shows a backbone r.m.s.d. of 2.35 Å. Despite different disulfide bond connectivities, the three μ-PIIIA isomer structures reveal a comparable flexibility and a solvent-exposed side chain for R14. This finding may explain their general ability to block VGSC $Na_V1.4$.

To better understand the results obtained herein we additionally performed molecular dynamic simulations for the three isomers when bound to $Na_V1.4$ (Supporting Information Figures S8–S12) based on the recently reported crystal structure of VGSC Na_VAB[18] (Supporting Information Figure S9). In accordance with the electrophysiological experiments, all three isomers blocked the $Na_V1.4$ channel pore during simulations (Figure 3, Supporting Information Figures S10–S12) and, more precisely, residue R14 of μ-PIIIA-1 binds much deeper in the pore than μ-PIIIA-2 and μ-PIIIA-3. Thus a deeper insertion of the toxin in the pore may be a key requirement for high affinity binding. Similarly, isomer-specific toxin binding to $Na_V1.4$ may explain the higher IC_{50} value of μ-PIIIA-1 compared to isomers **2** and **3**.

In any case, because the active μ-PIIIA isomers differ in fold only, and not by both primary amino acid sequence and conformation, these compounds represent exciting new tools for structure elucidation and investigation of the mode of action and function of voltage-gated ion channels. Since our findings represent unexpected and novel insights into the action of μ-conotoxins without modifying the chemical composition of these ligands, the results provide a strong incentive to intensify research focused on members of other conotoxin families as well.

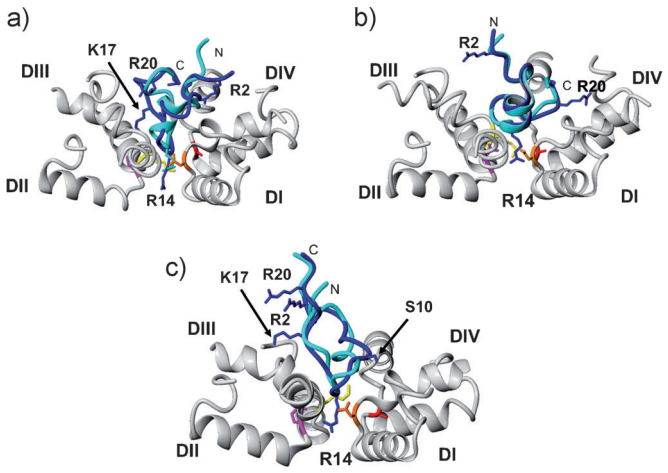

Figure 3. MD simulation of bound μ-PIIIA isomers: a) μ-PIIIA-1, b) μ-PIIIA-2, and c) μ-PIIIA-3 bound to the pore vestibule of $Na_V1.4$ (homology model based on VGSC Na_VAB[18]). For clarity, S5–S6 of DI–DIV are hidden. P-loops are shown in gray, with DEKA selective filter Asp400 (orange), Glu755 (magenta), Lys1237 (yellow), Ala1529 (red). Peptide structures (blue) represent conformations after MD simulation and initial structures (cyan) for μ-PIIIA-1, μ-PIIIA-2 (energy minimized NMR structures of these peptides), and for μ-PIIIA-3 (MD equilibrated structure after 5.85 ns of simulation). The r.m.s.d. of the corresponding structures is 5.26 Å (a), 2.89 Å (b), and 3.34 Å (c), respectively. Alignments were performed according to a multiple structure alignment algorithm (MUSTANG[19]) with YASARA.[20]

Received: October 4, 2011
Revised: December 22, 2011
Published online: March 12, 2012

Keywords: disulfide connectivity · NMR spectroscopy · structure–reactivity relationships · sodium channels · conotoxin

[1] F. H. Yu, W. A. Catterall, *Genome Biol.* **2003**, *4*, 207.1–207.7.
[2] a) J. N. Wood, J. P. Boorman, K. Okuse, M. D. Baker, *J. Neurobiol.* **2004**, *61*, 55–71; b) S. G. Waxman, *Nature* **2006**, *444*, 831–832; c) R. J. Lewis, C. I. Schroeder, J. Ekberg, K. J. Nielsen, M. Loughnan, L. Thomas, D. A. Adams, R. Drinkwater, D. J. Adams, P. F. Alewood, *Mol. Pharmacol.* **2007**, *71*, 676–685.
[3] H. Terlau, B. M. Olivera, *Physiol. Rev.* **2004**, *84*, 41–68.
[4] a) Q. Kaas, J. C. Westermann, D. J. Craik, *Toxicon* **2010**, *55*, 1491–1509; b) Q. Kaas, J. C. Westermann, R. Halai, C. K. Wang, D. J. Craik, *Bioinformatics* **2008**, *24*, 445–446.
[5] a) R. J. French, D. Yoshikami, M. F. Sheets, B. M. Olivera, *Mar. Drugs* **2010**, *8*, 2153–2161; b) R. B. Jacob, O. M. McDougal, *Cell. Mol. Life Sci.* **2010**, *67*, 17–27; c) R. A. Li, I. L. Ennis, R. J. French, S. C. Dudley, Jr., G. F. Tomaselli, E. Marban, *J. Biol. Chem.* **2001**, *276*, 11072–11077; d) J. R. McArthur, G. Singh, M. L. O'Mara, D. McMaster, V. Ostroumov, D. P. Tieleman, R. J. French, *Mol. Pharmacol.* **2011**, *80*, 219–227.
[6] K. J. Nielsen, M. Watson, D. J. Adams, A. K. Hammarstrom, P. W. Gage, J. M. Hill, D. J. Craik, L. Thomas, D. Adams, P. F. Alewood, R. J. Lewis, *J. Biol. Chem.* **2002**, *277*, 27247–27255.
[7] K. Wakamatsu, D. Kohda, H. Hatanaka, J. M. Lancelin, Y. Ishida, M. Oya, H. Nakamura, F. Inagaki, K. Sato, *Biochemistry* **1992**, *31*, 12577–12584.
[8] J. M. Hill, P. F. Alewood, D. J. Craik, *Biochemistry* **1996**, *35*, 8824–8835.
[9] D. W. Keizer, P. J. West, E. F. Lee, D. Yoshikami, B. M. Olivera, G. Bulaj, R. S. Norton, *J. Biol. Chem.* **2003**, *278*, 46805–46813.
[10] S. Yao, M. M. Zhang, D. Yoshikami, L. Azam, B. M. Olivera, G. Bulaj, R. S. Norton, *Biochemistry* **2008**, *47*, 10940–10949.
[11] K. K. Khoo, Z. P. Feng, B. J. Smith, M. M. Zhang, D. Yoshikami, B. M. Olivera, G. Bulaj, R. S. Norton, *Biochemistry* **2009**, *48*, 1210–1219.
[12] T. Kimura in *Houben-Weyl, Methods of Organic Chemistry, Synthesis of Peptides and Peptidomimetics, Vol. E22b* (Eds.: M. Goodman, A. Felix, L. Moroder, C. Toniolo), Thieme, Stuttgart, **2002**, pp. 142–161.
[13] J. L. Dutton, P. S. Bansal, R. C. Hogg, D. J. Adams, P. F. Alewood, D. J. Craik, *J. Biol. Chem.* **2002**, *277*, 48849–48857.
[14] a) E. Fuller, B. R. Green, P. Catlin, O. Buczek, J. S. Nielsen, B. M. Olivera, G. Bulaj, *FEBS J.* **2005**, *272*, 1727–1738; b) P. Safo, T. Rosenbaum, A. Shcherbatko, D. Y. Choi, E. Han, J. J. Toledo-Aral, B. M. Olivera, P. Brehm, G. Mandel, *J. Neurosci.* **2000**, *20*, 76–80; c) K. J. Shon, B. M. Olivera, M. Watkins, R. B. Jacobsen, W. R. Gray, C. Z. Floresca, L. J. Cruz, D. R. Hillyard, A. Brink, H. Terlau, D. Yoshikami, *J. Neurosci.* **1998**, *18*, 4473–4481.
[15] a) R. DeLa Cruz, F. G. Whitby, O. Buczek, G. Bulaj, *J. Pept. Res.* **2002**, *61*, 202–212; b) A. A. Miloslavina, E. Leipold, M. Kijas, A. Stark, S. H. Heinemann, D. Imhof, *J. Pept. Sci.* **2009**, *15*, 72–77; c) S. Zorn, E. Leipold, A. Hansel, G. Bulaj, B. M. Olivera, H. Terlau, S. H. Heinermann, *FEBS Lett.* **2006**, *580*, 1360–1364.
[16] L. Yu, C. Sun, D. Song, J. Shen, N. Xu, A. Gunasekera, P. J. Hajduk, E. T. Olejniczak, *Biochemistry* **2005**, *44*, 15834–15841.
[17] A. Lange, K. Giller, S. Hornig, M. F. Martin-Eauclaire, O. Pongs, S. Becker, M. Baldus, *Nature* **2006**, *440*, 959–962.
[18] J. Payandeh, T. Scheuer, N. Zheng, W. A. Catterall, *Nature* **2011**, *475*, 353–358.
[19] A. S. Konagurthu, J. C. Whisstock, P. J. Stuckey, A. M. Lesk, *Proteins Struct. Funct. Bioinf.* **2006**, *64*, 559–574.
[20] E. Krieger, T. Darden, S. B. Nabuurs, A. Finkelstein, G. Vriend, *Proteins Struct. Funct. Bioinf.* **2004**, *57*, 678–683.

